Chapter 40
Bayesian Prediction of Anxiety Level in Aged People at Rest Using 2-Channel NIRS Data from Prefrontal Cortex

Yukikatsu Fukuda, Wakana Ishikawa, Ryuhei Kanayama, Takashi Matsumoto, Naohiro Takemura, and Kaoru Sakatani

Abstract The aim of this study was to predict mental stress levels of aged people at rest from two-channel near-infrared spectroscopy (NIRS) data from the prefrontal cortex (PFC). We used the State-Trait Anxiety Inventory (STAI) for the mental stress index.

We previously constructed a machine learning algorithm to predict mental stress level using two-channel NIRS data from the PFC in 19 subjects aged 20–24 years at rest (Sato et al., Adv Exp Med Biol 765:251–256, 2013). In the present study, we attempted the same prediction for aged subjects aged 61–79 years (10 women; 7 men). The mental stress index was again STAI. After subjects answered the STAI questionnaire, the NIRS device measured oxy- and deoxy-hemoglobin concentration changes during a 3-min resting state. The algorithm was formulated within a Bayesian machine learning framework and implemented by Markov Chain Monte Carlo. Leave-one-subject-out cross-validation was performed.

Average prediction error between the actual and predicted STAI values was 5.27. Prediction errors of 12 subjects were lower than 5.0. Since the STAI score ranged from 20 to 80, the algorithm appeared functional for aged subjects also.

Keywords Anxiety • Near infrared spectroscopy • Prefrontal cortex • Bayesian regression • Aging

Y. Fukuda (✉) • W. Ishikawa • R. Kanayama • T. Matsumoto
Department of Electrical Engineering and Bioscience, Waseda University, Okubo 3-4-1, Nishiwaseda Campus Building 55th N-0402, Shinjuku-ku, Tokyo 169-0072, Japan
e-mail: yukikatsu_fukuda@fuji.waseda.jp

N. Takemura
Laboratory of Integrative Biomedical Engineering, Department of Electrical and Electronics Engineering, College of Engineering, Nihon University, Koriyama, Fukushima 963-8642, Japan

K. Sakatani
Department of Electrical and Electronics Engineering, Nihon University, Tokyo, Japan

H.M. Swartz et al. (eds.), *Oxygen Transport to Tissue XXXVI*, Advances in Experimental Medicine and Biology 812, DOI 10.1007/978-1-4939-0620-8_40,
© Springer Science+Business Media, LLC 2014

info.sk@ee.ce.nihon-u.ac.jp

1 Introduction

Recently, mental stress has become an important issue. However, measurements of mental stress have been based on experience, and a method of obtaining objective stress measurements will have huge potential in practical usage.

Research in this field has focused on the prefrontal cortex (PFC), which is an important area involved in stress responses. Davidson et al. reported that the asymmetry of PFC activities between the right and left hemispheres was related to emotional responses; specifically, right-dominant activity was induced when the subject was in a negative mood, and left-dominant activity was induced in a positive mood [1]. These emotional responses were also associated with stress responses. The laterality index showed right-dominant activity for stressful tasks and left-dominant activity for resting states [2]. Generally, fluctuations of NIRS data are thought to play an important role in predicting mental stress level, and a default-mode network works even when the subject is resting [3]; however, the detailed neurological and physiological systems lying behind this remain unclear. A statistical prediction method employing Bayesian regression with nonlinear regression models and Markov Chain Monte Carlo (MCMC) implementations has also been reported [4]. This method used NIRS data obtained from young subjects to predict State Trait Anxiety Inventory (STAI) scores.

In this paper, we applied the same framework to aged subjects to examine the effect of aging and to investigate the properties of this method. The evaluation criteria we employed were the root-mean-square error (RMSE), the correlation coefficient, and the p-value of a two-tailed t-test between the actual and predicted STAI values of aged subjects.

Because our experimental protocol was simple and the device could easily measure near-infrared spectroscopy (NIRS) data, this approach is promising for various applications, such as preventive medicine and environmental management, and will help us to understand cerebral physiological systems.

2 Materials and Methods

2.1 Experimental Settings

We measured NIRS data from 17 subjects (10 women; 7 men), aged 61–79 years. The subjects had no history of psychiatric or neurological disorders, and had completed informed consent forms approved by the ethics committee of the Nihon University School of Medicine prior to the study.

Each subject was seated upright in a comfortable chair with their eyes open, and a two-channel pocket NIRS system (PNIRS-10, Hamamatsu Photonics K.K., Japan) was mounted symmetrically on the forehead. The NIRS probes were positioned at the midpoint between the electrode positions Fp1/Fp3 (left) and Fp2/Fp4 (right) according to the international 10–20 system.

info.sk@ee.ce.nihon-u.ac.jp

Table 40.1 The features used in this study

No.	Variance	No.	Covariance	No.	Correlation coefficient
1	oxy(r)	5	oxy(r)/deoxy(r)	11	oxy(r)/deoxy(r)
2	deoxy(r)	6	oxy(r)/oxy(l)	12	oxy(r)/oxy(l)
3	oxy(l)	7	oxy(r)/deoxy(l)	13	oxy(r)/deoxy(l)
4	deoxy(l)	8	deoxy(r)/oxy(l)	14	deoxy(r)/oxy(l)
–	–	9	deoxy(r)/deoxy(l)	15	deoxy(r)/deoxy(l)
–	–	10	oxy(l)/deoxy(l)	16	oxy(l)/deoxy(l)

Oxy/deoxy denotes hemoglobin changes in the NIRS data, and letters "r" and "l" in parentheses denote the locations of the relevant channels. The numbers in the odd-numbered columns are feature numbers

Each subject performed one trial as described below:

Step 1. Answering STAI questionnaire. No time limit was set. The STAI results were used to measure the current anxiety level of the subjects.

Step 2. Preparation period (40 s). Subjects were allowed to move to make themselves comfortable, and the NIRS data became relatively steady within about 40 s. Parameters of the NIRS device were also set at the beginning of this period.

Step 3. Analysis period (3 min). Subjects were asked to remain relaxed and not to move during this period. No other instructions were given by the experimenters.

2.2 NIRS Data

The two-channel NIRS device acquired oxy- and deoxy-hemoglobin (Hb) concentrations. The data were a 4-dimensional matrix (right/left channels × oxy/deoxy-Hb) and 1,800 time-series values (180 s × 10 Hz sampling rate). We preprocessed the data to extract 16 second-order statistical features, namely, four variances, six covariances, and six correlation coefficients (Table 40.1). The second-order features were related in principle to the changes measured in the NIRS data.

2.3 Prediction

2.3.1 Prediction Flow

A leave-one-subject-out cross-validation (CV) was conducted. Of the NIRS and STAI datasets for the 17 subjects, one was reserved for testing, and the remaining 16 were used for training the machine. After parameters were learned with the training data, the reserved data were input to the machine for STAI prediction. One experiment consisted of repeating this procedure 17 times, once for each subject, and the final prediction results were averaged over the results of the five experiments.

info.sk@ee.ce.nihon-u.ac.jp

2.3.2 Prediction Algorithm

Let $x^{(i)} = (x_1^{(i)}, \ldots, x_K^{(i)}) \in R^K, i = \mathbf{1}, \ldots, N$, be the NIRS feature vector of the *i-th* individual and $y^{(i)}, i = \mathbf{1}, \ldots, N$, be the STAI state scores ($K = 3, N = \mathbf{17}$). We attempted to fit the data with the following learning model:

$$P\left(y^{(i)} \mid \boldsymbol{x}_t^{(i)}; \omega, \beta\right) = \sqrt{\frac{\beta}{2\pi}} \exp\left(-\frac{\beta}{2}\left(y^{(i)} - f\left(\boldsymbol{x}_t^{(i)}; \boldsymbol{\omega}\right)\right)^2\right) \tag{40.1}$$

where f is the basis function, and β is unknown hyperparameter, corresponding to the magnitude of uncertainty in the STAI scores. The relationship between the NIRS data and the STAI score is expected to be nonlinear, and therefore, we employed the nonlinear basis function:

$$f\left(\boldsymbol{x}_t^{(i)}; \boldsymbol{\omega}\right) := \sum_{h=1}^{H}\left[\omega_{(K+1)h}\,\sigma\left(\sum_{k=1}^{K}\left[\omega_{kh} x_{tk}^{(i)}\right] + \omega_{0h}\right)\right] + \omega_{(K+1)0} \tag{40.2}$$

where σ is a sigmoidal function that incorporates potential nonlinearities, and $\boldsymbol{\omega} = \{\omega_{kh}, \omega_{0h}, \omega_{(K+1)0}\}$, where $k = 1, \ldots, K$ and $h = 1, \ldots, H$ ($H = 8$) are the unknown parameters associated with the basis function. All unknown parameters $\boldsymbol{\omega}$ needed to be learned from the available data $\{x^{(i)}, y^{(i)}\}$. We formulated the prediction problem within a Bayesian framework, where a prior distribution was assumed about the unknown parameters incorporated into the data model in (40.1).

The prior distribution for $\boldsymbol{\omega}_k$ was $P(\boldsymbol{\omega}_k|\alpha_k) = \mathrm{N}(0, (1/\alpha_k)\boldsymbol{I})$, where $\mathrm{N}(0, (1/\alpha_k)\boldsymbol{I})$ denotes a Gaussian distribution with a mean of 0 and a covariance matrix $(1/\alpha_k)\boldsymbol{I}$, α_k is another hyperparameter to be learned, which often prevents overfitting, and $\boldsymbol{I}$ denotes the H-dimensional identity matrix. The prior distributions for α_k are set to the gamma distribution. Let $\boldsymbol{\alpha} = \{\alpha_k\}, \boldsymbol{x} = \{x_t^{(i)}\}$ and $\boldsymbol{y} = \{y^{(i)}\}$; then the Bayes formula gives the posterior distribution:

$$P\left(\boldsymbol{\omega}, \boldsymbol{\alpha} \mid \boldsymbol{x}, \boldsymbol{y}, \beta\right) \propto \prod_{t,j} P\left(y^{(i)} \mid \boldsymbol{x}_t^{(i)}; \boldsymbol{\omega}, \beta\right) P\left(\boldsymbol{\omega} \mid \boldsymbol{\alpha}\right) P\left(\alpha\right) \tag{40.3}$$

We used a Markov Chain Monte Carlo approximation to compute (40.3).

3 Results

We examined the prediction capability with all possible combinations of features in Table 40.1, that is, four variances, six covariances, and six correlation coefficients. For example, the number of combinations of correlation coefficients was $\Sigma_{n}{}^{6}{}_{=16}\mathrm{C}_n = 63$. The best performance was observed with feature vector (14, 15, 16). Figures 40.1 and 40.2 show the results obtained with these features.

info.sk@ee.ce.nihon-u.ac.jp

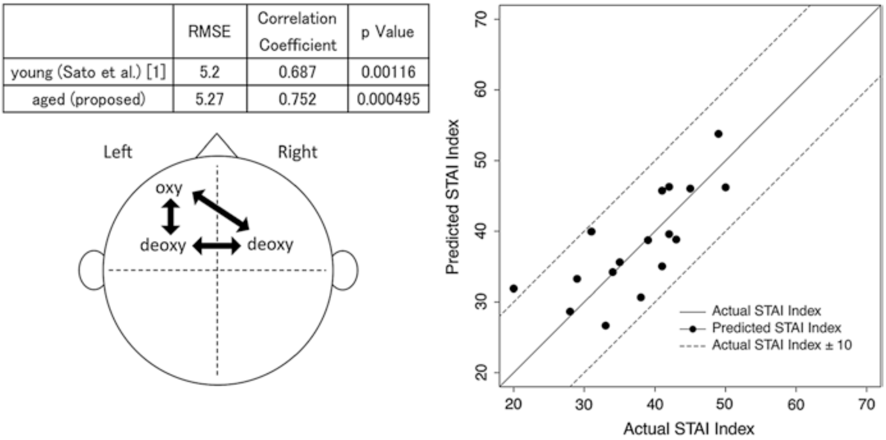

	RMSE	Correlation Coefficient	p Value
young (Sato et al.) [1]	5.2	0.687	0.00116
aged (proposed)	5.27	0.752	0.000495

Fig. 40.1 *Top-left* table shows the root-mean-square error, the Pearson correlation coefficient, and the p-value of two-tailed t-test across 17 subjects with the feature vector (14, 15, 16). *Bottom-left* illustration shows relations of NIRS data, consisting of the feature vector (14, 15, 16) in Table 40.1. *Right graph* shows scatter plot between Actual STAI and Predicted STAI scores. *Solid line* denotes Predicted STAI = Actual STAI, and *dotted lines* denote Actual STAI ± 10

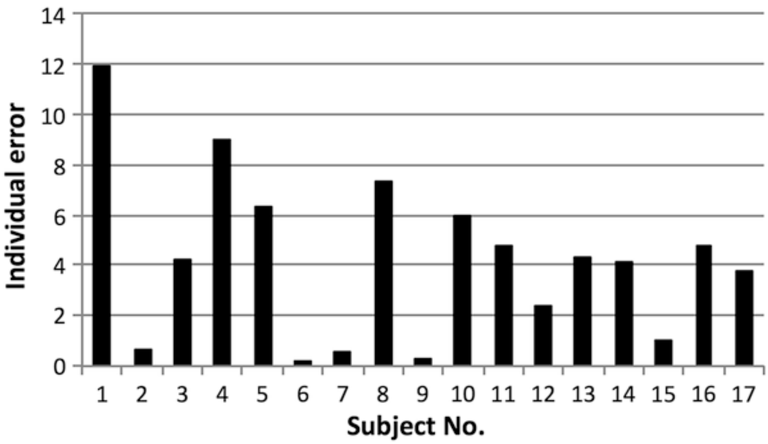

Fig. 40.2 Individual errors between the Actual STAI and Predicted STAI across 17 aged subjects with the feature vector (14, 15, 16) in Table 40.1

Figure 40.1, at the top-left, shows the average results of the 17 subjects, compared with the results of our previous study. The bottom-left illustration shows the sources of the feature vector (14, 15, 16): changes in left oxy-Hb, and changes in right and left deoxy-Hb. The right part in Fig. 40.1 shows a scatter plot of the actual STAI scores and the predicted STAI scores for all subjects, and Fig. 40.2 shows individual errors.

info.sk@ee.ce.nihon-u.ac.jp

As seen in the top-left table in Fig. 40.1, the difference between young and aged subjects does not appear to be large in terms of RMSE and the Pearson correlation coefficients.

4 Discussion

Stress response reflected in PFC activity is an active research topic. A statistical regression method of analyzing anxiety level in normal young subjects has been reported [4], but the reproducibility with other datasets remained unclear. Therefore, in the work described in this paper, we tested the same framework with normal aged subjects to examine the effect of aging.

For the individual errors shown in Fig. 40.2, 94 % were less than 10.0, whereas 70.5 % were less than 5.0. Observe that the lowest error was 0.216; however, the highest error was 12.0, which was relatively high, and this was observed at an STAI score of 20. This error was so high because such a low STAI score was observed in only one subject, and more data at low STAI scores will be needed to achieve higher accuracy. Recall that we conducted leave-one-subject-out cross-validation, and thus the STAI score for each subject was predicted with parameters trained using the data of 16 different subjects. Therefore, there is a possibility that common features may exist among subjects, namely, the feature vector (14, 15, 16) in Table 40.1, irrespective of the influence of in-born traits or grown-up personality on current anxiety level prediction.

Although prediction models in [4] and the present paper are the same, the associated parameters are different. In [4], features 11, 12 and mean of oxy(l) were extracted by ARD [5] whereas in this study, 14, 15 and 16 were chosen by an exhaustive search as described above so that the two predictors carry different parameter sets. Figure 40.1 appears to suggest that it could be worth studying the physiological meaning associated with the correlation between changes in left oxy-Hb and right/left deoxy-Hb.

References

1. Davidson R (1998) Anterior electrophysiological asymmetries, emotion, and depression: conceptual and methodological conundrums. Psychophysiology 35(05):607–614
2. Tanida M, Sakatani K, Takano R, Tagai K (2004) Relation between asymmetry of prefrontal corte activities and the autonomic nervous system during a mental arithmetic task: near infrared spectroscopy study. Neurosci Lett 369:69–74. doi:10.1016/j.neulet.2004.07.076
3. Greicius MD, Krasnow B, Reiss A, Menon V (2003) Functional connectivity in the resting brain: a network analysis of the default mode hypothesis. Proc Natl Acad Sci U S A 100:253–258
4. Sato M, Ishikawa W, Suzuki T, Matsumoto T, Tsujii T, Sakatani K (2013) Bayesian STAI anxiety index predictions based on prefrontal cortex NIRS data for the resting state. Adv Exp Med Biol 765:251–256. doi:10.1007/978-1-4614- 4989-8_35
5. Bishop C (2006) Pattern recognition and machine learning. Springer, Heidelberg

info.sk@ee.ce.nihon-u.ac.jp